Working memory circuitry in schizophrenia shows widespread cortical inefficiency and compensation

Miyoung A. Kim[a], **Emanuela Tura**[b], **Steven G. Potkin**[a], **James H. Fallon**[a], **Dara S. Manoach**[c], **Vince D. Calhoun**[d,e], **FBIRN**[f], and **Jessica A. Turner**[a,*]

[a] Department of Psychiatry and Human Behavior, University of California, Irvine, CA 92617

[b] Faculty of Medicine, University of British Columbia, Vancouver, BC V6T 1Z3

[c] Department of Psychiatry, Massachusetts General Hospital, and the Athinoula A. Martinos Center for Biomedical Imaging, Harvard Medical School, Boston MA

[d] The Mind Research Network, Albuquerque, NM 87131

[e] Department of ECE, University of New Mexico, Albuquerque, NM 87131

Abstract

Background—Working memory studies in schizophrenia (SZ), using functional magnetic resonance imaging (fMRI) and univariate analyses, have led to observations of hypo- or hyper-activation of discrete cortical regions and subsequent interpretations (e.g. neural inefficiencies). We employed a data-driven, multivariate analysis to identify the patterns of brain-behavior relationships in SZ during working memory.

Methods—fMRI scans were collected from 13 SZ and 18 healthy control (HC) participants performing a modified Sternberg item recognition paradigm with three memory loads. We applied partial least squares analysis (PLS) to assess brain activation during the task both alone and with behavioral measures (accuracy and response time, RT) as covariates.

Results—While the HC primary pattern was not affected by increasing load demands, SZ participants showed an exaggerated change in the Blood Oxygenation Level Dependent (BOLD) signal from the low to moderate memory load conditions and subsequent decrease in the greatest memory load, in frontal, motor, parietal and subcortical areas. With behavioral covariates, the separate groups identified distinct brain-behavior relationships and circuits. Increased activation of the middle temporal gyrus was associated with greater accuracy and faster RT only in SZ.

*Corresponding Author: Jessica Turner, Ph.D., 5251 California Avenue, Suite 240, Irvine, California, 92617, U.S.A., jessica.turner@uci.edu, (949) 824-3331 phone, (949) 824-3324 fax.
[f] www.fbirn.org

Conclusions—The inverted U-shaped curves in the SZ BOLD signal in the same areas that show flat activation in the HC data indicate wide-spread neural inefficiency in working memory in SZ. While both groups performed the task with similar levels of accuracy, participants with schizophrenia show a compensatory network of different sub-regions of the prefrontal cortex, parietal lobule, and the temporal gyri in this working memory task.

Keywords

Schizophrenia; working memory; functional magnetic resonance imaging; partial least squares; multivariate analysis; neurocircuitry

1. Introduction

Human working memory is mediated by a network of cortical regions, with dorsolateral prefrontal cortex (DLPFC) playing a critical role. Prefrontal activation and in particular DLPFC activation have been found to increase with the number of items being remembered (Braver, et al., 1997; Manoach, et al., 1997). Neuroimaging studies on working memory disruption in schizophrenia (SZ) have pointed to brain patterns that comprise hypo- (e.g. (Perlstein, et al., 2003)) and hyper-activation of various cortical and subcortical regions (e.g. (Mendrek, et al., 2005)). In schizophrenic patients, hypoactivation of the DLPFC, has been found repeatedly (e.g. (Barch, et al., 2003; Perlstein, et al., 2001)), and may be more pronounced at higher levels of working memory demand (Carter, et al., 1998), suggesting difficulty mobilizing neural resources for optimal task performance compared to healthy controls.

Others have observed a pattern of load-dependent DLPFC hyperactivation (Manoach, et al., 1997), i.e. brain response that is greater than matched control subjects. Manoach et al. (1999) attributed DLPFC hyperactivation in the context of poorer performance (i.e., less accurate and slower response time) in SZ to 'inefficiency'; that is, SZ need to devote greater cortical resources to perform the same task (Manoach, et al., 1999). Even those SZ participants who perform at relatively high levels of accuracy appear to utilize greater prefrontal resources while achieving lower accuracy in the higher memory loads than do healthy controls (HC) (Callicott, et al., 2000), supporting the notion of inefficient DLPFC activation in SZ.

However, the DLPFC is not the only area underlying SZ working memory deficits. Studies using other imaging and electrophysiological techniques, such as positron emissions tomography (PET) and electroencephalogram (EEG), suggest that the memory deficits in SZ are attributable to abnormal activation within DLPFC-involved functional cortical networks, notably fronto-temporal cortices. The temporal lobes, superior and inferior parietal lobes (Jansma, et al., 2004; Mendrek, et al., 2005; Quintana, et al., 2003), and basal ganglia (Manoach, et al., 2000) also have all been implicated in SZ dysfunction in different working memory tasks. A meta-analysis of N-back studies by Glahn et al., 2005 found consistent evidence for hypoactivation in DLPFC and other frontal cortical areas, as well as hyperactivation in the anterior cingulate, left frontal pole, right dorsomedial frontal cortex, leading to the argument that DLPFC dysfunction must be assessed within the function of the larger cortical networks (Glahn, et al., 2005).

Performance must be taken into account in the interpretation of circuitry differences in working memory (for reviews see (Manoach, 2003; Van Snellenberg, et al., 2006)). Some studies have found that controlling for performance removes any neuroimaging difference between chronic SZ and controls (Ramsey, et al., 2002), while others have found that the differences persist (e.g. (Cannon, et al., 2005; Koch, et al., 2008; Potkin, et al., 2009)) or that new areas of hypo- or hyper activation are revealed (Johnson, et al., 2006). On a wide range of working memory tasks SZ perform more slowly than HC (Brown, et al., 2009; Manoach, et al., 1999). The

increase in RT for verbal working memory has been correlated with increased activation of bilateral posterior parietal areas in HC (Honey, et al., 2000); however, this link was absent in SZ, supporting the idea of a loss of fronto-parieto network function in SZ (Honey, et al., 2002). This was partially supported by a recent SIRP task analysis by Brown and colleagues finding greater correlations between BOLD signal changes and RT increases in healthy subjects than in subjects with schizophrenia, though their findings were in frontal and subcortical, rather than parietal regions (Brown, et al., 2009).

To further identify the neural circuitry of working memory and the covariations with the observed behavioral deficits in SZ, we used partial least squares (PLS; (McIntosh, et al., 1996; Wold, 1966)), a whole-brain multivariate analysis, on a subset of the data from (Potkin, et al., 2009) and (Brown, et al., 2009). When applied to neuroimaging data, PLS identifies highly salient and specific coherence patterns in the BOLD (blood-oxygen-level dependent) signal across the brain, revealing task-dependent changes in activity, brain-behavior relationships, and possible functional connectivity of various regions (McIntosh and Lobaugh, 2004). We sought to identify the primary patterns of activated brain regions that distinguished between SZ and HC with increasing working memory demands, and covaried with performance. The purpose of this study was to confirm findings of hyperactivity in the DLPFC in this task and to identify whether that hyperactivity is shown in other regions, while allowing for novel disease-specific, performance-related circuitry.

2. Materials and Methods

2.1 Participants

Thirteen SZ participants and 18 HC participants gave informed consent prior to enrolling in the multi-site Functional Imaging Biomedical Informatics Research Network (FBIRN) Phase II Study at the University of California, Irvine (UCI); the study was conducted with approval from UCI's Institutional Review Board (IRB). To minimize the possible confounding effects of multiple site data collection, including the strength of the MRI scanner, we chose to focus only on the UCI data for this analysis. Clinical participants were chronic patients (i.e. duration of illness > 2 years) and diagnosed using the Structured Clinical Interview for Diagnosis (SCID) (First, et al., 2002) according to the criteria of the Diagnostic Standards Manual IV (DSM-IV) for SZ or schizoaffective disorder. The two participant groups were matched for age within two years. Additional group demographic profiles and clinical measures, including the median scores for the Scale for Assessment of Negative Symptoms (SANS) (Andreasen, 1984a) and the Scale for Assessment of Positive Symptoms (SAPS) (Andreasen, 1984b), are shown in Table 1. Other inclusion/exclusion and clinical participants' psychiatric medication information is listed in Supplemental Material 1.

2.2 Data collection and image processing

The imaging data were collected on a 1.5T Marconi (Picker) MRI scanner at the UCI Research Imaging Center. A more detailed description of the scanning session is provided in Supplemental Material 1 (and in (Brown, et al., 2009)). The functional imaging scans were preprocessed for motion detection and correction, using the SPM2 software (University College, London; http://www.fil.ion.ucl.ac.uk/spm/software/spm2/). The scans were then co-registered and normalized to a Montreal Neurological Institute (MNI, Quebec, Canada) brain template, and smoothed with an 8mm FWHM 3D Gaussian filter (Friston, 1995a; Friston, 1995b). The resulting images served as the source for the PLS analyses.

2.3 Working Memory task: SIRP

The experimental design included six conditions: three memory loads (1, 3, and 5 items) by two conditions or epochs (encode and probe). In a modified SIRP task (adapted from (Manoach,

et al., 1999)), participants were presented with a set of target digits to remember during the encode epoch (6s), followed immediately by the probe epoch (38s) in which they indicated with a button press whether or not each probe digit presented was a member of the target set. All three working memory load conditions were presented twice within each of the three runs of the task in a pseudorandom order, and accuracy and RT were recorded (see Supplemental Material 1 and refer to (Potkin, et al., 2009) or (Brown, et al., 2009)).

2.4 Statistical Analysis: Behavioral and Imaging Data

2.4.1 Behavioral Data—We performed mixed-effects analyses of variance (ANOVA) to test the effects of diagnosis, working memory load, and any interactions on accuracy and RT from each participant. RT data from one of the HC was not collected; we used the scores from 17 of the 18 HC (and 13 SZ) for the analysis.

2.4.2 Imaging Data: PLS on SIRP Task and Behavior—For a more comprehensive explanation of PLS, refer to Supplemental Material 1. Analogous to principal or independent components analyses, PLS decomposes the data and task covariance matrix into latent variables (LVs), which comprise an LV profile, a singular value, and a brain image. The LV's identify the primary patterns in the data across the different conditions, and the brain regions which show those patterns (through being positively weighted on the LV profile), or which show the opposite of those patterns (through being negatively weighted). Using the PLS software (http://www.rotman-baycrest.on.ca/pls, Version 5.0910261), analyses were performed on the task conditions alone (*task PLS analysis*), and with accuracy and RT as covariates (*behavior PLS analyses*). The task analysis examined the differences in BOLD signal changes from baseline during the six conditions (three loads by two epochs) in SZ and HC; the behavior analyses examined the relationship between each individual's accuracy/RT and the BOLD signal changes during the same conditions. While the participant's accuracy and RT are measured only during the probe epoch, activation of areas showing a positive correlation with accuracy during encode may predict performance in the subsequent probe epoch. We also performed the same analyses within the HC and SZ datasets separately, and found the same patterns as in the combined analysis. Those comparison results are presented in Supplement 6.

The number of permutations was set at 1000 iterations and bootstrapping at 200 to ensure reliability of the analyses. For each analysis, PLS identified 12 latent variables (LV) – only those with $p \leq 0.05$ by permutation testing are reported; in identifying voxels that show the pattern identified in the LV, the bootstrap ratio (BSR) threshold was set at ± 3.5 (Table 2). The BSR for a voxel is the ratio of the voxel salience to its estimated standard error, and serves as the measure of the reliability of the measure (see Supplemental Material 1).

3. Results

3.1 Behavioral Data

Error rates increased with increasing working memory load ($F(2,56) = 5.7, p < 0.01$); although HC on average outperformed SZ on each load, the difference was not statistically significant (Figure 1a). There was no significant load by diagnosis interaction in accuracy. RT increased with load ($F(2,56) = 132.6, p < 0.01$); again although HC on average were faster than SZ on each load, the difference was not statistically significant (Figure 1b). There was, however, a significant interaction between load and diagnosis on RT ($F(2,56) = 9.1, p < 0.001$), with the two groups being similar at the lowest load but SZ showing a greater increase in RT with increased load.

3.2 Imaging Data and LV's

We present selected significant LV's with the most significant brain clusters; all significant LV's (p ≤ 0.05) are presented in Supplemental Material 2. Listings of activated areas corresponding to each significant LV profile are presented in Table 2 (abridged for cluster size ≥ 100 voxels) and comprehensively in Supplemental Material 3 and 4 by PLS analysis/LV and by brain regions, respectively. Supplemental Material 5 provides a more thorough examination of the patterns found in each brain lobe and hemisphere across all PLS analyses. Areas positively weighted on an LV are represented in red on the image slices (e.g. Figure 2a) and those negatively weighted are in blue.

3.2.1 Task PLS Analysis—The pattern of LV1 (Figure 2b) identifies the distinction between the encode and probe conditions for all three loads as the primary source of covariance in the task-dependent brain activity (approximately 36% of the covariance). For areas which are positively weighted on this latent variable (those shown in red in Figure 2a), activity during probe epochs is greater than during encode epochs. The reverse is true for areas which are negatively weighted on this variable (shown in blue in Figure 2a)—they show a greater BOLD signal change during encode than probe conditions.

The pattern also shows that while HC have the same pattern overall regardless of load (as shown in the dotted lines in Figure 2b), SZ show relatively greater activation for the 3 item memory load than for 1 or 5, and an overall increase from 1 to 5 items (solid lines). An analysis of variance (ANOVA) on the participants' brain scores, showing the variation across subjects and conditions, showed that probe scores were greater than encode (p < 0.05), and both the effects of load and the interaction between load and diagnosis were significant, with SZ showing significantly lower values at load 1, and an increase for load 3 that HC did not. The largest cluster that was positively weighted on this LV was the left postcentral gyrus (BA 3), spreading into precentral gyrus, supplementary motor areas (SMA), the postcentral gyrus and inferior parietal lobe (BA 40); the greatest negatively correlated area was the right calcarine/lingual gyrus (BA 17/18) (Figures 2a and 2b).

The pattern of LV3 (Figure 2c, 15% covariance) shows a weaker encode/probe distinction and increasing activation with increasing load in both groups in the positively weighted brain areas. The greatest areas positively correlated with this LV were in the right and left middle frontal gyri (BA 46/10) (see Table 2, and Supplemental Material 3 and 4).

Task PLS analyses performed on HC and SZ separately revealed similar LV's and corresponding brain activation patterns that confirmed the results from the combined group analysis (see Figure 1 of Supplemental Material 6). The primary LV pattern (LV1, 50% covariance) of the HC group alone showed the encode/probe separation, and a moderate decrease with increasing memory load; while the primary LV pattern of the SZ group (50% covariance) showed a rather dramatic increase from load 1 to 3 and a moderate decrease from load 3 to 5, and the secondary LV pattern of the SZ group (25% covariance) showed the encode/probe distinction with a slight increase from load 1 to 3 and a moderate decrease from load 3 to 5. Thus, while the results are not identical when the groups are analyzed separately, the separate analyses showed similar patterns and areas supporting those patterns to those identified in the combined analysis; for brevity, we will focus on the interpretation of the combined analysis.

3.2.2. Behavior PLS Analysis - Accuracy as a Covariate—The first LV using accuracy as a covariate accounts for 36% of the covariance, and shows reliable patterns for SZ data only (see Figure 3a). The pattern of LV1 shows that SZ's accuracy for loads 1 and 5, in particular, was positively correlated with activation of the left middle temporal gyrus (BA 21/22) and bilateral middle temporal gyri (BA 21). SZ's accuracy was negatively correlated with the

activation of the left caudate nucleus, on the other hand, along with the right superior temporal gyrus and left occipital areas, particularly for loads 1 and 5 (see Table 2, and Supplemental Material 3 and 4).

In contrast to LV1, the pattern of LV2 (15% of the covariance; Figure 3b) indicates areas in which accuracy in HC was positively correlated with increased activation in the mid- and high-level loads, while SZ showed a more variable but decreasing pattern. The activation of the left middle frontal gyrus (BA 46) and the left inferior temporal gyrus (BA 37/19) was positively weighted on this pattern. In contrast to LV1 in SZ, HC's accuracy was negatively correlated with activation in the right middle temporal gyrus (BA 21) and the left superior temporal gyrus (BA 22/42). DLPFC, along with the activation of the inferior temporal gyrus (BA 37/19) and globus pallidus, contributed to the accuracy of the more challenging loads (3 and 5) in HC, whereas the middle temporal gyrus (BA 21) and the superior temporal gyrus (BA 22/42) had a similar effect for load 5 in SZ. Separate analyses within each group also showed the same patterns (results not shown).

3.2.3. Behavior PLS Analysis - RT as a Covariate—In Figure 4a, left and right graphs show the RT analysis first latent variable patterns for SZ and HC separately (23% of the covariance). Again, this LV identifies reliable patterns in the SZ data only. LV1 (Figure 4a, left) showed RT positively correlating (i.e. slower RT) in the SZ data with increased activation in non-dominant motor planning areas, such as the right precentral gyrus (BA 6), the right SMA (BA 6), and the left superior frontal gyrus (BA 8). Faster RT was positively correlated with increased activation in the areas showing negative weightings on this LV: the left inferior temporal gyrus (BA 20), the right inferior frontal triangular cortex (bordering BA 45/46), the bilateral superior parietal lobule (BA 40), the right inferior parietal lobule (also BA 40), and bilateral middle frontal gyrus (BA 9).

LV 3 (15% of the covariance; Figure 4b) identified areas which showed opposite effects on RT in SZ and HC, particularly at the higher memory loads: Negatively weighted areas (left cuneus (BA 8) and right middle temporal gyrus (BA 21) showed a negative correlation with RT (more activation sped up RT) in the SZ data, while showing a positive correlation with (slower) RT in the HC data.

A separate analysis explored the relationship between the areas identified as related to RT and accuracy, which is reported in Supplemental Material 3, Section 2. This analysis identified that the only area showing any evidence of a speed-accuracy trade-off was the right inferior frontal areas (BA 45) in the SZ data, where increased activation was correlated with increased speed at the expense of accuracy. The right middle temporal area was also identified as being correlated with both accuracy and RT in the SZ data, but in contrast to the frontal area, the areas were correlated with both increased speed and increased accuracy. See Supplemental Material 5 for an overview of all brain regions and analyses.

4. Discussion

These analyses confirm the presence of concurrent hypoactivations and hyperactivations of various brain regions during a working memory task in SZ, attesting to the complexity of the relationship between the functional response of the schizophrenic brain and various components of working memory, such as memory load, the relationship to behavior, and the difference between encode and probe conditions. The primary finding identified during our SIRP task (Task PLS, LV1 – Figure 2) revealed that in the probe condition, while SZ significantly under-utilized neural resources for the lowest memory load compared to HC, they showed hyperactivation significantly for the moderate load, which then tapered off in the highest memory load to equal that of HC. I.e., while HC did not exhibit a relationship between

activation and load during either probe or encode conditions, SZ in the probe condition showed a steep positive relationship with increasing load from low to moderate levels, but a negative relationship from moderate to high load. We interpret this exaggerated increase in response for the same task response as cortical inefficiency, supporting what was seen in the DLPFC analysis of (Potkin, et al., 2009). In the encode conditions, in contrast, areas which were positively activated were hypoactive in the higher loads, in keeping with (Johnson, et al., 2006) and (Schlosser, et al., 2008).

Meta-analyses of results obtained from the neuroimaging literature, particularly those that used the N-back paradigm exclusively, have previously found lateral premotor, SMA, dorso- and ventrolateral premotor, posterior parietal and inferior parietal areas involved in working memory processing in HC data (e.g. (Owen, et al., 2005)). The SIRP, with a clear separation between the learning phase of the working memory process and the maintenance and retrieval phases, differs dramatically from the n-back in its cognitive demands. However, we find similar networks of areas in the HC encode and probe data as found in (Owen, et al., 2005). What we see in the activation pattern of the precentral and postcentral gyri, putamen and cerebellum, increasing together with BA 9, 46, and 40 during memory retrieval and identification in the probe condition, is as expected (Cairo, et al., 2004; Rypma and D'Esposito, 1999; Walter, et al., 2007).

The neural inefficiency we find in SZ during the probe condition, obviously, is not limited to the DLPFC. SZ also appear to show this pattern of hypo- then hyper-activity with increasing load in large regions of motor, pre-motor, frontal, parietal, and basal ganglia areas. This includes both the lateral PFC (BA 46/10) and the inferior parietal lobule (BA 40), which is in keeping with previous findings in SZ during memory retention, e.g., (Quintana, et al., 2003). Hyperactivity in these fronto-parietal regions during specifically performance-matched n-back tasks has also been found previously (Thermenos, et al., 2005), although parietal hyperactivations did not survive the meta-analysis of the n-back paradigm in SZ as summarized in (Glahn, et al., 2005). This is also in keeping with the Independent Components Analysis by Kim et al. (2009) (Kim, et al., 2009a) of a similar SIRP dataset (of which our SIRP data were not a part), which identified that SZ showed greater activation during the probe than encode conditions, and during the medium load level in many of these same areas. These observations, combined with the aforementioned findings about the DLPFC, indicate that a broad network of regions appears to exhibit an inverted-U shape in their activations for SZ during working memory maintenance and retrieval.

The results do not indicate a strong inverted-U in the healthy control subjects within these memory load levels. Our findings do not rule out the possibility of cortical regions increasing activation with memory load in HC, but if such increases exist in these conditions, they do not account for the maximal covariance in these data. Indeed, the third latent variable in the task analysis showed areas which increase with memory load in both groups, but this was a much weaker effect and not the primary pattern. However, the memory load in this study was not particularly demanding for healthy controls. It is below the levels used in (Johnson, et al., 2006), for example, in which healthy controls showed strong increases with memory load in many cortical regions in both encode and retrieval. The increase in their study began at a 5 item load, at which point the SZ participants were no longer showing any increases.

The larger multi-site study of which these data are a part (Potkin, et al., 2009) primarily analyzed the mean activation over all of BA 9/46, and found hyper-activation in the mid-level memory demands for SZ. Our analysis highlights the regional and sub-regional variations within this larger prefrontal region. In the Task analysis, areas within bilateral BA 46 showed a dramatic positive change in activation from load 1 to 3 in SZ, while HC effectively showed no significant change in activation from load 1 to 3 (Figure 2a). However, different sub-regions

of bilateral BA 9 and 46 showed a uniform increase in activation with increasing load in both HC and SZ groups (Figure 2c). These supports the idea that there might be sub-regional, patterns of activation in both that are both task- and load-dependent in the DLPFC (as suggested by (Manoach, 2003)).

While hyperactivation in SZ in areas that HC also commonly use for the task—i.e., using the same region but more actively to perform the task as well or worse than HC—can be interpreted as inefficiency, finding activation in a cortical area that is related only to SZ performance can be interpreted as indicating compensation (as suggested in (Quintana, et al., 2003; Ragland, et al., 2007)). Our second overall finding is the diagnosis-specific relationships between task performance and BOLD signal changes across the brain. The fact that the extracted LV's were reliable for the SZ participants separately from the HC subjects, for both accuracy and RT, supports the idea that the two groups are recruiting very different areas in different ways to perform the working memory task. We find that activations in the DLPFC, the left inferior temporal lobe, and the inferior parietal lobe are positively correlated with accuracy in healthy participants, while the participants with schizophrenia recruit a range of areas, including the inferior rather than dorsolateral frontal gyri and regions throughout the temporal lobe for increased accuracy or faster response times. This recruitment of areas not related to the task in the HC data suggests a compensatory mechanism involving a distinct circuitry unique to SZ.

The interpretation of this study is limited to chronic SZ, and the effects of antipsychotic medication must be considered. The relationships between the caudate nucleus activations and performance in particular should be tested in subjects whose medications do not affect basal ganglia volume and function. Previous studies have reported on individual fMRI maps of unmedicated patients being similar to medicated patients, however (Callicott, et al., 1998), and if anything medication can normalize brain activations rather than exacerbate them (Ramsey, et al., 2002). The siblings of patients can show similar working memory hyperactivations as patients do (Callicott, et al., 2003) as well, suggesting that these findings are not driven by medication.

These analyses implicated much of right and left temporal lobes as having distinct relationships with performance in the HC and SZ groups. The middle temporal gyrus was engaged for increased accuracy in SZ (positively weighted on LV1 and negatively weighted on LV2 and LV4); simultaneously, this area was also correlated with RT, however, oppositely in the two groups (negatively weighted for RT LV3 in SZ, Figure 4b) under the greater loads. These findings suggest that SZ activated the bilateral middle temporal gyrus significantly for increased accuracy on the majority of the loads (Figures 3a and 3b), and used the right middle temporal gyrus extensively for a more rapid response to the task (Figure 4b).

The middle temporal gyrus is known to be affected volumetrically in patients with both first-episode and chronic schizophrenia (Kuroki, et al., 2006; Onitsuka, et al., 2004). Its function has been implicated in maintenance during phonological working memory in HC (Strand, et al., 2008). Furthermore, comprehension of language appears to be disrupted in persons with lesions to the middle temporal gyrus (Dronkers, et al., 2004), suggesting its mediating role in verbal working memory. More recently, it has been linked to a processing deficit in the detection of auditory oddball stimuli in SZ patients (Kim, et al., 2009b), possibly refining the role of the middle temporal area and its response to auditory stimuli in SZ. Similar areas can also be hyperactivated with increased demand during word tasks in SZ (Ragland, et al., 2008). Our findings in the middle and inferior temporal gyri are complementary to a recent work showing that when SZ performed *incorrectly* on a similar Sternberg task, there was hypo-activation in inferior temporal areas relative to HC (Koch, et al., 2009). Given these results, we surmise that SZ access these temporal areas as compensation under increasing demand to accomplish comparable levels of accuracy and RT to those of HC in this memory task. How

the activation pattern of this seemingly crucial brain region covaries with the other regions associated with working memory and contributes to behavior remains to be investigated, underscoring further the need to examine brain activation patterns in the context of circuitries rather than as discrete units alone.

Supplementary Material

Refer to Web version on PubMed Central for supplementary material.

Acknowledgments

References

Andreasen, NC. Modified Scale for the Assessment of Negative Symptoms (SANS). University of Iowa; Iowa City, IA: 1984a.

Andreasen, NC. Scale for the Assessment of Positive Symptoms (SAPS). University of Iowa; Iowa City, IA: 1984b.

Barch DM, Sheline YI, Csernansky JG, Snyder AZ. Working memory and prefrontal cortex dysfunction: specificity to schizophrenia compared with major depression. Biological psychiatry 2003;53(5):376–384. [PubMed: 12614990]

Braver TS, Cohen JD, Nystrom LE, Jonides J, Smith EE, et al. A parametric study of prefrontal cortex involvement in human working memory. NeuroImage 1997;5(1):49–62. [PubMed: 9038284]

Brown GG, McCarthy G, Bischoff-Grethe A, Ozyurt B, Greve D, et al. Brain-performance correlates of working memory retrieval in schizophrenia: a cognitive modeling approach. Schizophr Bull 2009;35 (1):32–46. [PubMed: 19023127]

Cairo TA, Liddle PF, Woodward TS, Ngan ET. The influence of working memory load on phase specific patterns of cortical activity. Brain research 2004;21(3):377–387. [PubMed: 15511653]

Callicott JH, Bertolino A, Mattay VS, Langheim FJ, Duyn J, et al. Physiological dysfunction of the dorsolateral prefrontal cortex in schizophrenia revisited. Cereb Cortex 2000;10(11):1078–1092. [PubMed: 11053229]

Callicott JH, Egan MF, Mattay VS, Bertolino A, Bone AD, et al. Abnormal fMRI response of the dorsolateral prefrontal cortex in cognitively intact siblings of patients with schizophrenia. Am J Psychiatry 2003;160(4):709–719. [PubMed: 12668360]

Callicott JH, Ramsey NF, Tallent K, Bertolino A, Knable MB, et al. Functional magnetic resonance imaging brain mapping in psychiatry: methodological issues illustrated in a study of working memory in schizophrenia. Neuropsychopharmacology 1998;18(3):186–196. [PubMed: 9471116]

Cannon TD, Glahn DC, Kim J, Van Erp TG, Karlsgodt K, et al. Dorsolateral prefrontal cortex activity during maintenance and manipulation of information in working memory in patients with schizophrenia. Archives of general psychiatry 2005;62(10):1071–1080. [PubMed: 16203952]

Carter CS, Perlstein W, Ganguli R, Brar J, Mintun M, et al. Functional hypofrontality and working memory dysfunction in schizophrenia. Am J Psychiatry 1998;155(9):1285–1287. [PubMed: 9734557]

Dronkers NF, Wilkins DP, Van Valin RD Jr, Redfern BB, Jaeger JJ. Lesion analysis of the brain areas involved in language comprehension. Cognition 2004;92(1–2):145–177. [PubMed: 15037129]

First, MB.; Spitzer, RL.; Gibbon, M.; Williams, JBW. Research Version, Patient Edition. (SCID-I/P) Biometrics Research. New York State Psychiatric Institute; New York: 2002. Structured Clinical Interview for DSM-IV-TR Axis I Disorders.

Friston KJ, Ashburner J, Frith CD, Poline J-B, Heather JD, Frackowiak RSJ. Spatial registration and normalization of images. Human brain mapping 1995a;2:165–189.

Friston KJ, Holmes AP, Worsley KJ, Poline JB, Frith CD, Frackowiak RSJ. Statistical Parametric Maps in functional imaging: A general linear approach. Human brain mapping 1995b;2:189–210.

Glahn DC, Ragland JD, Abramoff A, Barrett J, Laird AR, et al. Beyond hypofrontality: a quantitative meta-analysis of functional neuroimaging studies of working memory in schizophrenia. Human brain mapping 2005;25(1):60–69. [PubMed: 15846819]

Honey GD, Bullmore ET, Sharma T. Prolonged reaction time to a verbal working memory task predicts increased power of posterior parietal cortical activation. NeuroImage 2000;12(5):495–503. [PubMed: 11034857]

Honey GD, Bullmore ET, Sharma T. De-coupling of cognitive performance and cerebral functional response during working memory in schizophrenia. Schizophr Res 2002;53(1–2):45–56. [PubMed: 11728837]

Jansma JM, Ramsey NF, van der Wee NJ, Kahn RS. Working memory capacity in schizophrenia: a parametric fMRI study. Schizophr Res 2004;68(2–3):159–171. [PubMed: 15099600]

Johnson MR, Morris NA, Astur RS, Calhoun VD, Mathalon DH, et al. A functional magnetic resonance imaging study of working memory abnormalities in schizophrenia. Biological psychiatry 2006;60 (1):11–21. [PubMed: 16503328]

Kim DI, Manoach DS, Mathalon DH, Turner JA, Mannell M, et al. Dysregulation of working memory and default-mode networks in schizophrenia using independent component analysis, an fBIRN and MCIC study. Human brain mapping. 2009a

Kim DI, Mathalon DH, Ford JM, Mannell M, Turner JA, et al. Auditory oddball deficits in schizophrenia: an independent component analysis of the fMRI multisite function BIRN study. Schizophr Bull 2009b;35(1):67–81. [PubMed: 19074498]

Koch K, Wagner G, Nenadic I, Schachtzabel C, Schultz C, et al. Fronto-striatal hypoactivation during correct information retrieval in patients with schizophrenia: an fMRI study. Neuroscience 2008;153 (1):54–62. [PubMed: 18359576]

Koch K, Wagner G, Schultz C, Schachtzabel C, Nenadic I, et al. Altered error-related activity in patients with schizophrenia. Neuropsychologia. 2009

Kuroki N, Shenton ME, Salisbury DF, Hirayasu Y, Onitsuka T, et al. Middle and inferior temporal gyrus gray matter volume abnormalities in first-episode schizophrenia: an MRI study. Am J Psychiatry 2006;163(12):2103–2110. [PubMed: 17151161]

Manoach DS. Prefrontal cortex dysfunction during working memory performance in schizophrenia: reconciling discrepant findings. Schizophr Res 2003;60(2–3):285–298. [PubMed: 12591590]

Manoach DS, Gollub RL, Benson ES, Searl MM, Goff DC, et al. Schizophrenic subjects show aberrant fMRI activation of dorsolateral prefrontal cortex and basal ganglia during working memory performance. Biological psychiatry 2000;48(2):99–109. [PubMed: 10903406]

Manoach DS, Press DZ, Thangaraj V, Searl MM, Goff DC, et al. Schizophrenic subjects activate dorsolateral prefrontal cortex during a working memory task, as measured by fMRI. Biological psychiatry 1999;45(9):1128–1137. [PubMed: 10331104]

Manoach DS, Schlaug G, Siewert B, Darby DG, Bly BM, et al. Prefrontal cortex fMRI signal changes are correlated with working memory load. Neuroreport 1997;8(2):545–549. [PubMed: 9080445]

McIntosh AR, Bookstein FL, Haxby JV, Grady CL. Spatial pattern analysis of functional brain images using partial least squares. NeuroImage 1996;3(3 Pt 1):143–157. [PubMed: 9345485]

McIntosh AR, Lobaugh NJ. Partial least squares analysis of neuroimaging data: applications and advances. NeuroImage 2004;23(Suppl 1):S250–263. [PubMed: 15501095]

Mendrek A, Kiehl KA, Smith AM, Irwin D, Forster BB, et al. Dysfunction of a distributed neural circuitry in schizophrenia patients during a working-memory performance. Psychological medicine 2005;35 (2):187–196. [PubMed: 15841676]

Onitsuka T, Shenton ME, Salisbury DF, Dickey CC, Kasai K, et al. Middle and inferior temporal gyrus gray matter volume abnormalities in chronic schizophrenia: an MRI study. Am J Psychiatry 2004;161 (9):1603–1611. [PubMed: 15337650]

Owen AM, McMillan KM, Laird AR, Bullmore E. N-back working memory paradigm: a meta-analysis of normative functional neuroimaging studies. Human brain mapping 2005;25(1):46–59. [PubMed: 15846822]

Perlstein WM, Carter CS, Noll DC, Cohen JD. Relation of prefrontal cortex dysfunction to working memory and symptoms in schizophrenia. Am J Psychiatry 2001;158(7):1105–1113. [PubMed: 11431233]

Perlstein WM, Dixit NK, Carter CS, Noll DC, Cohen JD. Prefrontal cortex dysfunction mediates deficits in working memory and prepotent responding in schizophrenia. Biological psychiatry 2003;53(1): 25–38. [PubMed: 12513942]

Potkin SG, Turner JA, Brown GG, McCarthy G, Greve DN, et al. Working memory and DLPFC inefficiency in schizophrenia: the FBIRN study. Schizophr Bull 2009;35(1):19–31. [PubMed: 19042912]

Quintana J, Wong T, Ortiz-Portillo E, Kovalik E, Davidson T, et al. Prefrontal-posterior parietal networks in schizophrenia: primary dysfunctions and secondary compensations. Biological psychiatry 2003;53 (1):12–24. [PubMed: 12513941]

Ragland JD, Moelter ST, Bhati MT, Valdez JN, Kohler CG, et al. Effect of retrieval effort and switching demand on fMRI activation during semantic word generation in schizophrenia. Schizophr Res 2008;99(1–3):312–323. [PubMed: 18155880]

Ragland JD, Yoon J, Minzenberg MJ, Carter CS. Neuroimaging of cognitive disability in schizophrenia: Search for a pathophysiological mechanism. International Review of Psychiatry 2007;19(4):417–427. [PubMed: 17671874]

Ramsey NF, Koning HA, Welles P, Cahn W, van der Linden JA, et al. Excessive recruitment of neural systems subserving logical reasoning in schizophrenia. Brain 2002;125(Pt 8):1793–1807. [PubMed: 12135970]

Rypma B, D'Esposito M. The roles of prefrontal brain regions in components of working memory: effects of memory load and individual differences. Proceedings of the National Academy of Sciences of the United States of America 1999;96(11):6558–6563. [PubMed: 10339627]

Schlosser RGM, Koch K, Wagner G, Nenadic I, Roebel M, et al. Inefficient executive cognitive control in schizophrenia is preceded by altered functional activation during information encoding: An fMRI study. Neuropsychologia 2008;46:336–347. [PubMed: 17707869]

Strand F, Forssberg H, Klingberg T, Norrelgen F. Phonological working memory with auditory presentation of pseudo-words -- an event related fMRI Study. Brain Res 2008;1212:48–54. [PubMed: 18442810]

Thermenos HW, Goldstein JM, Buka SL, Poldrack RA, Koch JK, et al. The effect of working memory performance on functional MRI in schizophrenia. Schizophr Res 2005;74(2–3):179–194. [PubMed: 15721998]

Van Snellenberg JX, Torres IJ, Thornton AE. Functional neuroimaging of working memory in schizophrenia: task performance as a moderating variable. Neuropsychology 2006;20(5):497–510. [PubMed: 16938013]

Walter H, Vasic N, Hose A, Spitzer M, Wolf RC. Working memory dysfunction in schizophrenia compared to healthy controls and patients with depression: evidence from event-related fMRI. NeuroImage 2007;35(4):1551–1561. [PubMed: 17363277]

Wold, H. Estimation of principal components and related models by iterative least squares. In: Krishnaiah, PR., editor. Multivariate Analysis. Academic Press; New York: 1966.
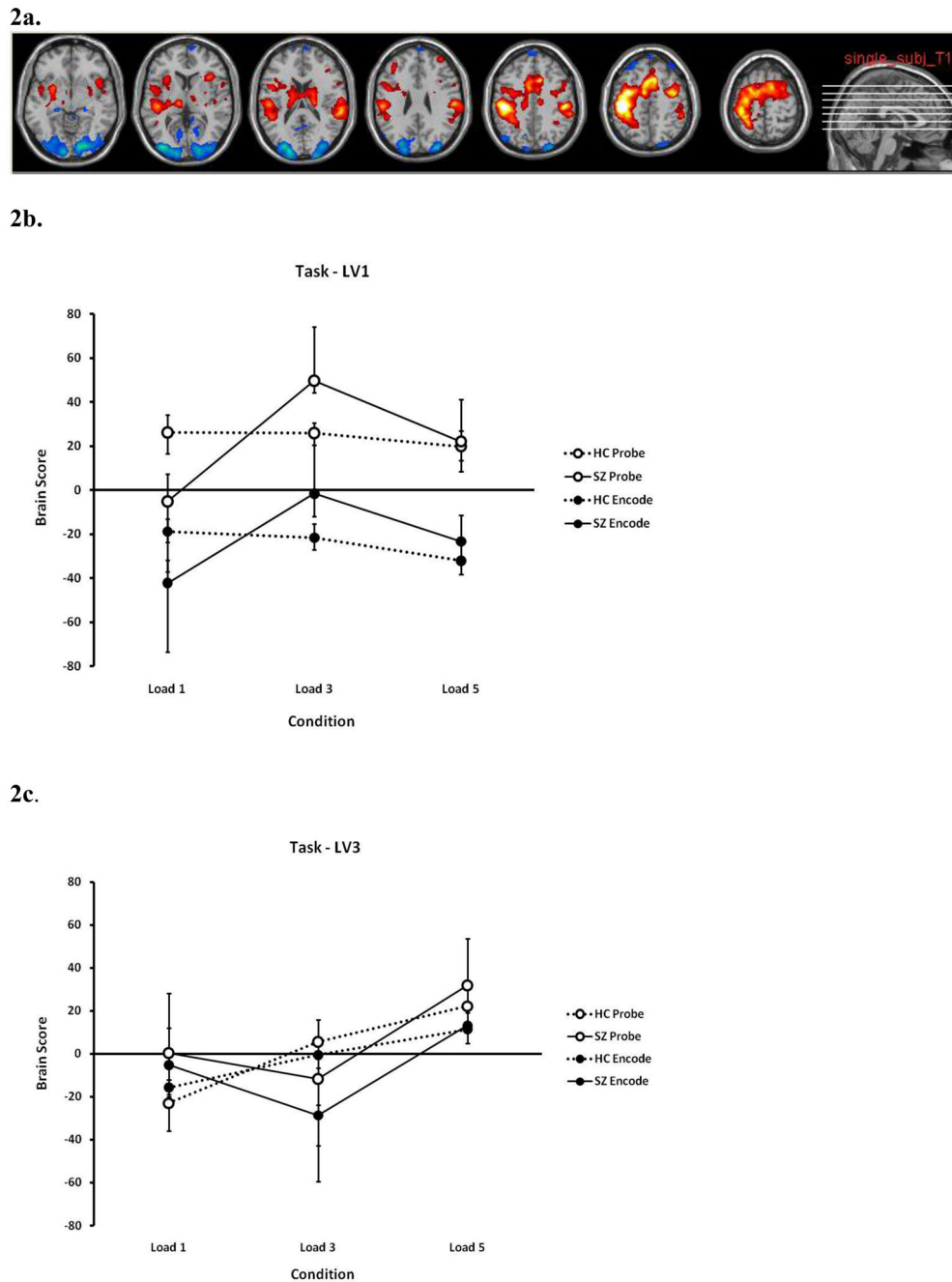
1a.
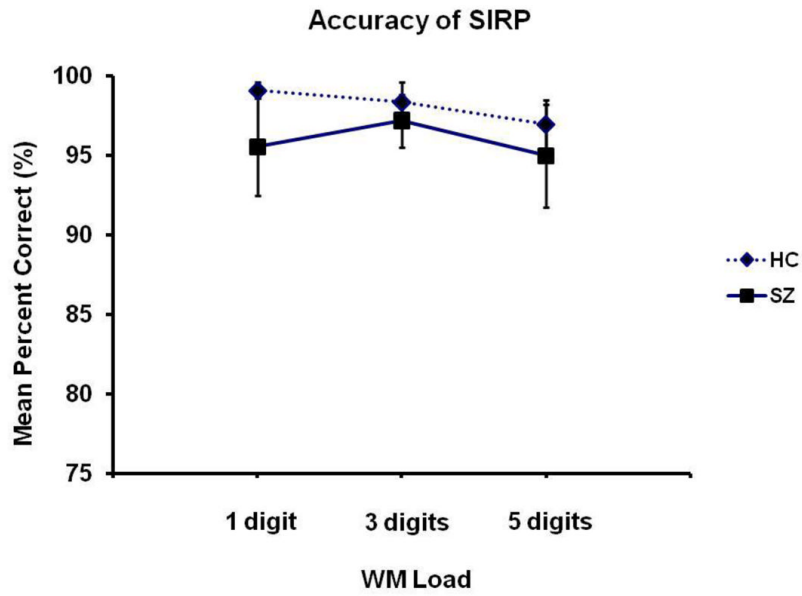
1b.
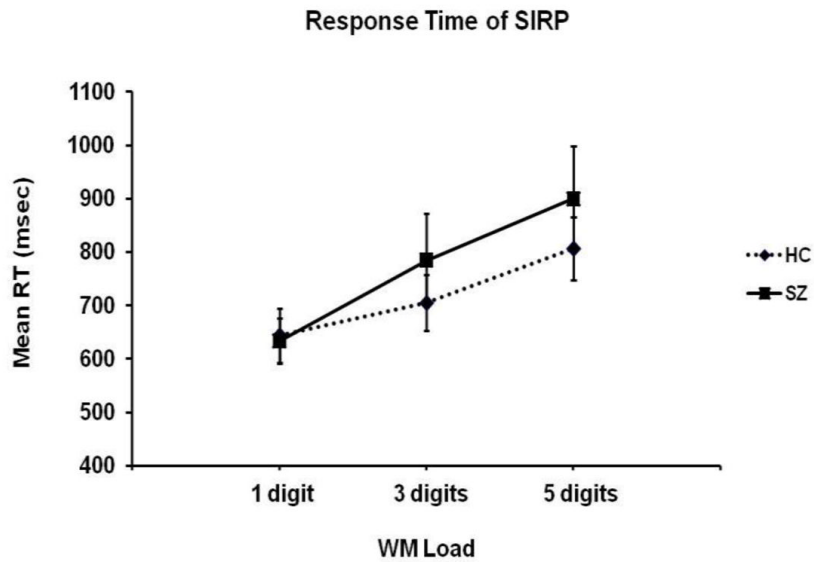
Figure 1.
Performance measures for schizophrenia (SZ) and healthy control (HC) participants. Accuracy decreased with increasing number of items to remember, or working memory (WM) load, in both groups (1a). Response time (RT) slowed with load (WM) in both groups, with the SZ group showing a greater effect (1b).

2a.

2b.

2c.

Figure 2.
Brain areas (2a) and brain score profiles for latent variables 1 (LV1) (2b) and LV3 (2c) in the
Task Partial Least Squares (PLS) analysis. The areas indicated in Figure 2a are the areas which
show the profile of Figure 2b. In both 2b and 2c, dashed lines indicate healthy controls (HC)
and solid lines indicate schizophrenia (SZ) participants; closed circles indicate the encode
conditions and open circles indicate the probe conditions. LV1 showed the distinction between
areas specific to encode or probe conditions, and indicated the neural ineffiency in SZ through
the hyperactivation in the moderate memory load conditions. See text for more description.
See Table 2 and Supplemental Material 3 – 5 for full listings and further discussion of brain
regions which were positively or negatively weighted on the various LV's.

3a.
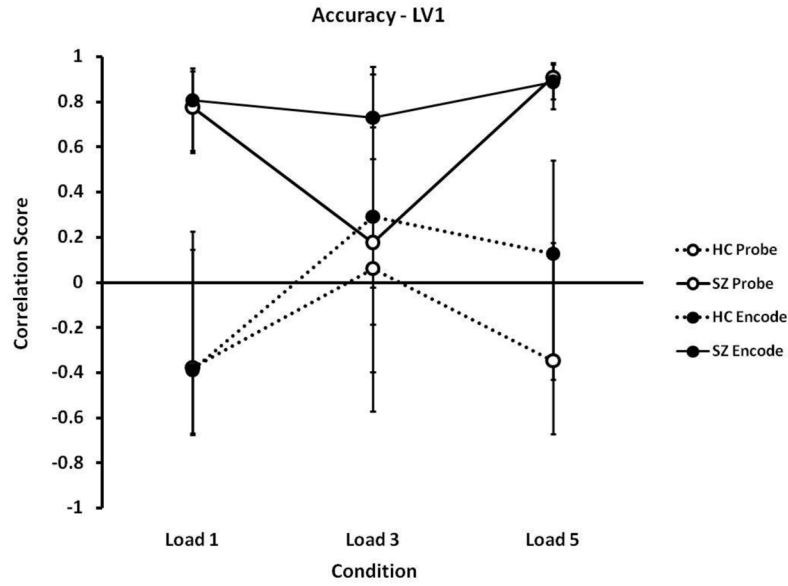
3b.
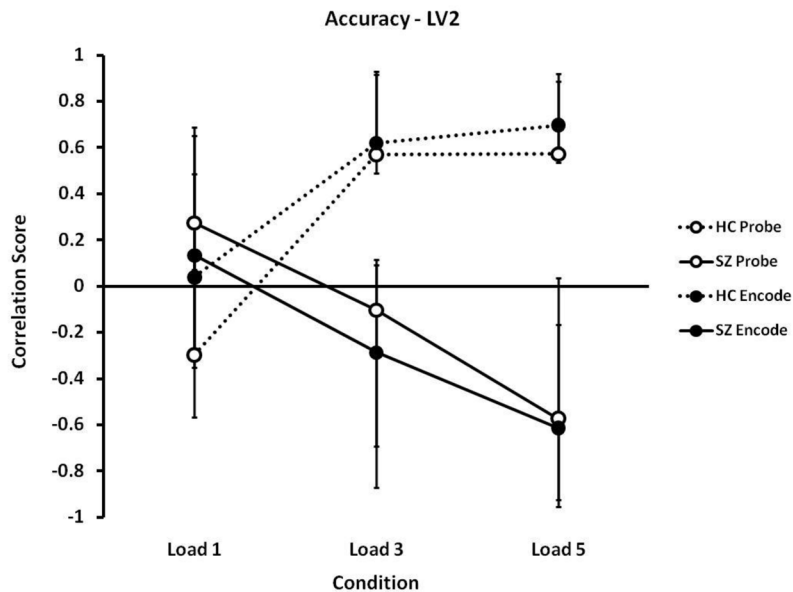
Figure 3.
Correlation score profiles for latent variable 1 (LV1) (3a) and LV2 (3b) in the Behavior Partial Least Squares (PLS) analysis for accuracy. Dashed lines indicate healthy controls (HC) and solid lines indicate schizophrenia (SZ) participants; closed circles indicate the encode conditions and open circles indicate the probe conditions. LV1 showed a strong positive correlation between accuracy of working memory loads 1 and 5 in SZ group and the activated areas (namely the middle temporal gyrus, BA 21), while no such strong correlation was observed in the HC group (3a); in LV2, accuracy in the two groups depended heavily on different brain regions for the higher loads, suggesting the possible involvement of different circuits for each group (3b).

4a.
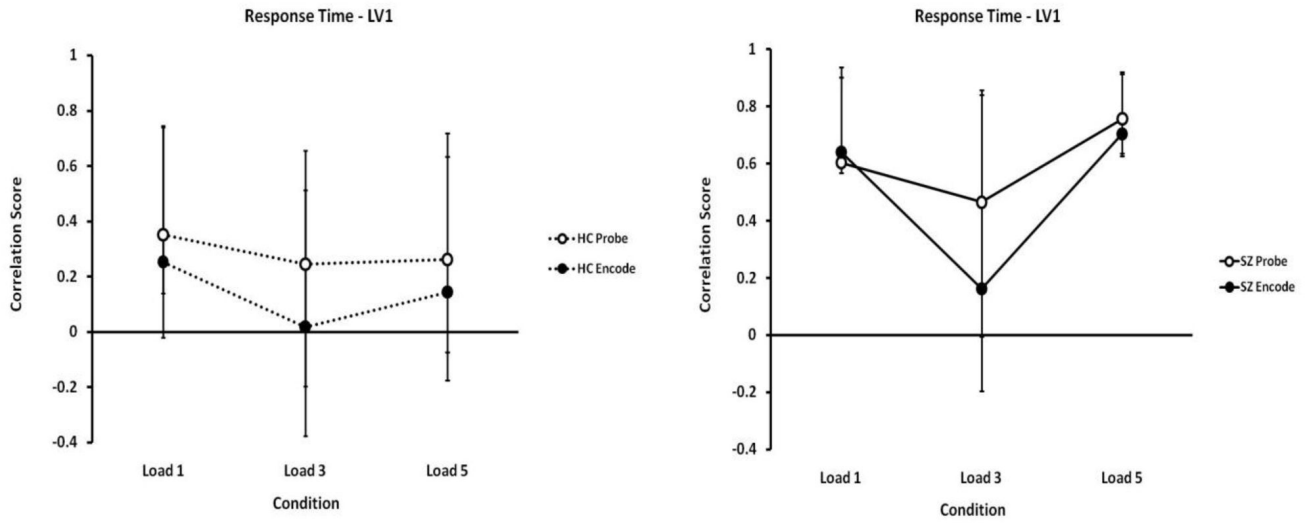
4b.
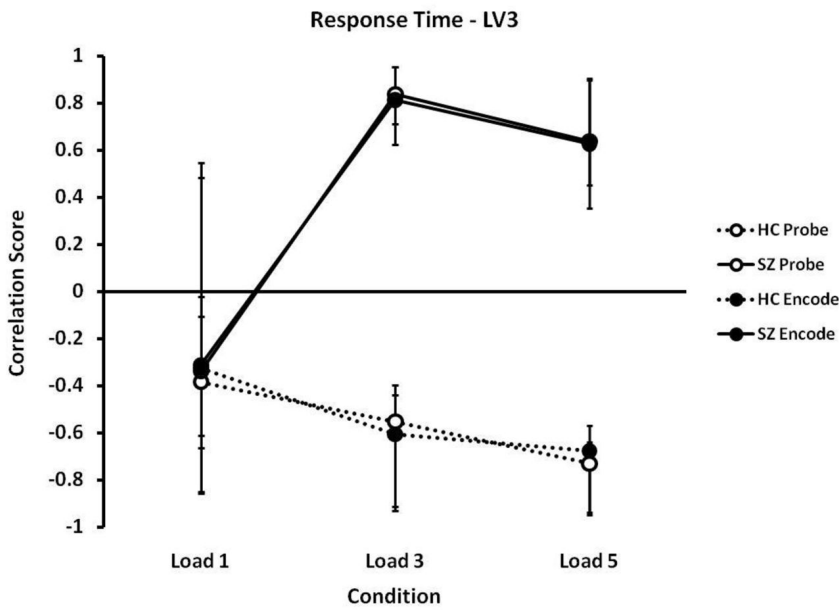
Figure 4.
Correlation score profiles for latent variable 1 (LV1) (4a – left, HC data; right, SZ data) and LV3 (4b) in the Behavior Partial Least Squares (PLS) analysis for response time (RT). Dashed lines indicate healthy controls (HC) and solid lines indicate schizophrenia (SZ) participants; closed circles indicate the encode conditions and open circles indicate the probe conditions. A strong positive correlation with RT existed across all working memory loads in the SZ group in LV1 (4a – right), while no reliable correlation was observed in the HC group (4a – left). LV3 showed that RT was dependent on different circuits in the two groups, especially for the greater loads (4b).

Table 1

Participant demographic, clinical, and behavioral data by group.

	SZ	HC
Number of Participants	13	18
Male : Female	10 : 3	13 : 5
Mean age ± SD, in years	41 ± 10	41 ± 11
Right-Handedness, in percent	84.6	83.3
Mean Education of Participant ± SD, in years	11.8 ± 1.1	14.9 ± 2.5
Mean Education of Caretaker(s) ± SD, in years:		
Primary Caretaker	13.1 ± 3.5	12.9 ± 2.6
Secondary Caretaker	13.0 ± 3.7	12.7 ± 3.3
DSM-IV Diagnosis (number of participants)	295.3 (7) 295.9 (1) 295.7 (5)	N/A
Median score of Scale for Assessment of Negative Symptoms (SANS)	10.0 [a]	N/A
Median score of Scale for Assessment of Positive Symptoms (SAPS)	6.5 [b]	N/A
Mean Global Assessment for Functioning (GAF)	57.5 [c]	N/A

[a] median SANS score from 11 out of 13 schizophrenia (SZ) participants

[b] median SAPS score from 12 out of 13 SZ participants

[c] mean GAF score from 11 out of 13 SZ participants

HC = healthy control participants

SD = standard deviation

Table 2

Prominently activated brain areas identified by the two most significant latent variables in each partial least squares (PLS) analysis. In Task PLS (Table 2a) and Behavior PLS analyses for accuracy (Table 2b) and response time, RT (Table 2c), we include the maximal voxel locations represented in terms of Brodmann area (BA), Montreal Neurological Institute (MNI) coordinates, cluster size (≥ 100 voxels), and bootstrap ratio (BSR) set at ± 3.5. All other significant LV's are listed in Supplemental Material 3 and 4.

a.

LV	Brain Lobe	Hemi	Brain Region	BA	MNI Coordinates (x y z)	Cluster Size (voxels)	BSR
			TASK PLS ANALYSIS				
1	Parietal	Left	Postcentral gyrus	3	−48 −26 44	19838	15.5
1	Parietal	Right	Postcentral gyrus	3	48 −24 42	2854	9.7
1		Right	Putamen		30 −4 −2	864	6.4
1		Right	Cerebellum		4 −64 −16	109	5.8
1	Frontal	Right	Middle frontal gyrus	46	34 50 28	130	5.3
1	Frontal	Left	Middle frontal gyrus	46	−38 38 30	160	5.0
1	Occipital	Right	Lingual gyrus (borders cerebellum)	27	8 −44 0	110	−4.6
1	Parietal	Left	Angular gyrus	39	−46 −74 40	170	−5.0
1	Frontal	Left	Superior frontal gyrus	9	−24 42 50	113	−5.0
1	Occipital	Right	Calcarine	17	12 −88 −2	4547	−9.8
1	Occipital	Left	Middle occipital	18	−40 −88 8	4051	−10.0
3	Frontal	Right	Middle frontal gyrus	46/10	40 58 10	594	6.9
3	Frontal	Left	Middle frontal gyrus	46/10	−40 60 10	254	5.6
3	Frontal	Right	Middle frontal orbital	11	6 30 −12	111	−4.7

b.

LV	Brain Lobe	Hemi	Brain Region	BA	MNI Coordinates (x y z)	Cluster Size (voxels)	BSR
			BEHAVIOR PLS ANALYSIS (Accuracy)				
1	Temporal	Left	Middle temporal gyrus	21/22	−60 −46 4	318	8.7
1	Temporal	Right	Middle temporal gyrus	21	60 −38 −2	249	6.5
1	Temporal	Left	Middle temporal gyrus	21	−60 −20 −12	113	6.4
1	Occipital	Left	Middle occipital gyrus	39	−46 −80 20	120	−4.9
1		Left	Caudate nucleus		−14 22 4	247	−5.2
1	Temporal	Right	Superior temporal gyrus	48	50 0 −2	236	−6.4
1	Occipital	Left	Cuneus		−10 −68 28	195	−6.5

b.

LV	Brain Lobe	Hemi	Brain Region	BA	MNI Coordinates (x y z)	Cluster Size (voxels)	BSR
2	Frontal	Left	Middle frontal gyrus	46	−34 60 26	318	5.9
2		Right	Globus pallidus		16 −10 −8	153	5.6
2	Temporal	Left	Inferior temporal gyrus	37/19	−54 −70 −6	312	5.3
2		Left	Superior temporal gyrus	22/42	−66 −36 14	346	−5.5
2	Temporal	Right	Middle temporal gyrus	21	68 −34 0	396	−6.0

c.

LV	Brain Lobe	Hemi	Brain Region	BA	MNI Coordinates (x y z)	Cluster Size (voxels)	BSR
			BEHAVIOR PLS ANALYSIS (RT)				
1	Parietal	Right	Supplementary motor area (SMA)	6	14 −6 64	491	5.5
1	Frontal	Right	Precentral gyrus	6	38 −12 52	582	5.4
1	Frontal	Left	Superior frontal gyrus	8	−22 8 52	154	4.9
1	Parietal	Left	Superior parietal lobule	40	−40 −52 60	102	−5.5
1	Frontal	Right	Inferior frontal triangular	45	46 46 2	183	−6.3
1	Temporal	Left	Inferior temporal gyrus	20	−68 −40 −12	116	−7.2
3	Temporal	Right	Middle temporal gyrus	21	64 −48 −4	199	−5.2
3	Occipital	Left	Cuneus/calcarine	18	−16 −90 14	287	−6.1